water

MDPI

Article

TiO_2 Doped with Noble Metals as an Efficient Solution for the Photodegradation of Hazardous Organic Water Pollutants at Ambient Conditions

Amalia Maria Sescu [1], Lidia Favier [2,*], Doina Lutic [3], Nicolas Soto-Donoso [2,4,5], Gabriela Ciobanu [1] and Maria Harja [1,*]

[1] Faculty of Chemical Engineering and Environmental Protection, "Gheorghe Asachi" Technical University of Iasi, 700050 Iasi, Romania; sescu.amaliamaria@gmail.com (A.M.S.); gciobanu@tuiasi.ro (G.C.)
[2] Ecole Nationale Supérieure de Chimie de Rennes, University of Rennes, CNRS, ISCR—UMR6226, F-35000 Rennes, France; nicolas.soto.d@usach.cl
[3] Faculty of Chemistry, "Alexandru Ioan Cuza" University of Iasi, 700506 Iasi, Romania; doilut@uaic.ro
[4] Facultad de Química y Biología, Universidad de Santiago de Chile, Santiago 9170022, Chile
[5] Centro para el Desarrollo de la Nanociencia y Nanotecnología, CEDENNA, Universidad de Santiago de Chile, Santiago 9170022, Chile
* Correspondence: lidia.favier@ensc-rennes.fr (L.F.); mharja@tuiasi.ro (M.H.); Tel.: +33-223-238-135 (L.F.); +40-0747909645 (M.H.)

Abstract: This work highlights new insights into the performance of TiO_2 doped with noble metal catalysts for the photocatalytic degradation of organic water pollutants. Different samples of titanium dioxide doped with noble metals (Au and Pd) were successfully synthesized via incipient wet impregnation (IWI) and ultrasound-assisted impregnation (US) methods. X-ray diffraction, scanning electron microscopy and UV-Vis reflectance spectroscopy were used for the characterization of the obtained materials. Their photocatalytic efficiency was investigated in aqueous suspension thorough a series of laboratory tests performed under ultraviolet (UV-A) irradiation conditions using 2,4 dinitrophenol (2,4 DNP) as a target molecule. The results clearly show that the method used for the catalyst synthesis affects its photocatalytic activity. It was found that the samples prepared by the IWI method exhibited high photocatalytic activity, and the removal rate obtained with TiO_2-Pd/IWI was higher than that found for TiO_2-Au/IWI. Furthermore, for the best catalyst, some extra photocatalytic experiments were conducted with rhodamine 6G (R6G), a highly stable molecule with a very different chemical structure to 2,4 DNP, in order to check the reactivity of this material. Moreover, the recycling experiments carried out with TiO_2-Pd/IWI clearly demonstrated the high photocatalytic stability of this material for the degradation of 2,4 DNP. All of the collected data confirmed the interesting photocatalytic potential of the selected catalyst in the elimination of organic pollutants with no obvious change in its reactivity after four reaction cycles, which is very promising for promoting future applications in water depollution.

Keywords: degradation; noble metal doping; persistent organic pollutants; photocatalysis; titanium dioxide

check for updates

Citation: Sescu, A.M.; Favier, L.; Lutic, D.; Soto-Donoso, N.; Ciobanu, G.; Harja, M. TiO_2 Doped with Noble Metals as an Efficient Solution for the Photodegradation of Hazardous Organic Water Pollutants at Ambient Conditions. *Water* **2021**, *13*, 19. https://dx.doi.org/10.3390/w13010019

Received: 16 November 2020
Accepted: 18 December 2020
Published: 24 December 2020

Publisher's Note: MDPI stays neutral with regard to jurisdictional claims in published maps and institutional affiliations.

Copyright: © 2020 by the authors. Licensee MDPI, Basel, Switzerland. This article is an open access article distributed under the terms and conditions of the Creative Commons Attribution (CC BY) license (https://creativecommons.org/licenses/by/4.0/).

1. Introduction

Fast industrial development and human activities cause major damages to the environment because of the release of harmful organic pollutants. Most of these pollutants are recognized for their toxicity, mutagenicity and carcinogenicity, representing a major ecological concern [1]. In this context, over the last decades, an increasing interest among scientists has emerged regarding the development of new technologies in the area of water and wastewater treatment with the aim of enhancing the elimination of organic compounds and, thus, reducing their impact on the aquatic system.

Heterogeneous photocatalysis is an advanced oxidation process that has many applications for the pollution abatement. This oxidation process is recognized today as a

very promising, green and easy-to-apply strategy regarding the effective degradation of stable organic molecules from wastewater and industrial effluents [2–4]. Briefly, in a photocatalytic reaction, a semiconductor interacts with photons that have sufficient energy in order to promote an electron from the valence band to the conduction band, followed by the generation of reactive oxidizing species (often hydroxyl radicals) from water. In many studies, hydroxyl radicals, HO·, are typically reported as very reactive species which are able to degrade and mineralize organic pollutants, transforming them into harmless products, such as CO_2 and H_2O [5–7]. Among these semiconductor materials, titanium dioxide (TiO_2) was widely used in many photocatalytic applications because of its low toxicity, chemical stability, availability, convenient physical and optical properties, and low cost [8,9]. Numerous works recognized TiO_2-based heterogeneous photocatalysis as an efficient technology for the elimination of different organic pollutants from water [10–12]. However, an important drawback in its use is related to the high recombination rate (within nanoseconds) of charge carries, which limits its photocatalytic efficiency [13]. A possible way to overcome it is to promote the charge carrier separation, reducing the recombination rate of the photo-generated electrons and holes, thus improving its photocatalytic efficiency [14]. One of the strategies considered as useful for improving the TiO_2 activity is doping with noble metals [15–17]. The effect of noble metal loading (Au, Ag and Pt) on the surface of different commercial TiO_2 was investigated in some previous studies for the photodegradation of different organic molecules [16,18–21]. For example, for TiO_2 doping with platinum, the photocatalytic effect does not always cause an increase in the activity. Furthermore, the detailed procedure of doping significantly influences the photocatalyst efficiency.

A detailed literature study was performed in order to investigate the roles and the performance enhancements caused by noble metal doping of titanium oxide supports by applying different preparation methods. The literature mentions various doping procedures, such as the sol–gel method [22], ultrasound treatment followed by UV irradiation [23], different versions of impregnation techniques of commercial titania [24,25], photodeposition from noble metal salt solutions [26,27], and radiolysis [28]. Some examples of noble metal-doped TiO_2 by various preparation techniques with applications in the photocatalytic decomposition of organic molecules are displayed in Table 1.

Table 1. Photocatalytic performance of noble metal-doped TiO_2.

Material	Preparation Procedure	Reaction Conditions	Elimination Efficiency	Ref
Mesoporous TiO_2 doped with Pd and Au	Sol-gel	Simulated wastewater with 8.71 mg/L Total Organic Carbon (TOC), 15 W UV lamp	93% (Au/TiO2)	[22]
Pd-, Pt-, Ag- or Cu-doped TiO2 (P-25)	US treatment and UV light in water-propanol	2,2′,4,4′-tetrabromodiphenyl ether, 300 W UV lamp	100% on 5%Pd-TiO_2	[23]
0.5% Pt/P-25 10% Ag/P-25	Impregnation from polyol solutions under reflux	Dichloroacetic acid (DCA), 150 W UV lamp	70%, 62% t-BuOH in 5 h *	[24]
1%Pt/TiO_2/SiO_2 (a)1%Pd/TiO_2/SiO_2 (b)1%Ag/TiO_2/SiO_2	Photodeposition in acetic acid suspensions of TiO_2/SiO_2 containing $PdCl_2$ or $H_2PtCl_6 \cdot 6H_2O$ under UV (8 W lamp) for 15 h	Brilliant red (K-2G), cationic blue (CBX), 300 W UV lamp	K-2G 280% rate increase on (a), 30% rate increase on (b)	[26]
0.5% and 1% Ag and Pt/P-25	Photodeposition in methanol (Ag) and oxalic acid solution (Pt) under UV-C (4W lamp) for 5 h	Oxalic acid, 9 W UV-A lamp	70–85% on doped samples, 40% on P-25	[27]
0.1% Ag and/or 0.1% Pd and Pt/P-25	Radiolysis	Toluene phenol, 63 mW UV-LED, or Vis-LED	50–97% or 60–100% depending on the doping	[28]
TiO_2 and Pd/TiO_2	Sol-gel method (Ti isopropoxide and Pd nitrate)	Methylene blue, methyl orange, 100 W UV lamp	83.4 and 75.3% mineralization after 180 min	[29]

* Best yields were obtained in t-BuOH decomposition.

The information gathered in Table 1 reveals the large diversity of materials and their tremendous versatility as photocatalytic materials. Simple organic compounds, such as alcohols, acids, and quinones, as well as dyes, and even complex mixtures of dissolved organic compounds simulating real wastewater have been subjected to photocatalytic processes to obtain the deep cleaning thereof. We must underline that in most cases, the reactions are possible due to the use of considerably powerful UV lamps that are necessary in the processes, thereby causing electrical energy consumption and limiting application at a larger scale. Therefore, in most research on the topics of photocatalytic water cleaning, irradiation durations of up to of 120 min are considered reasonable for a reaction in order to be taken into account as a convenient time value for a practical process.

In this work, two different preparation methods, the incipient wet impregnation (IWI) and the ultrasound-assisted (US) impregnation, were employed for the preparation of the doped TiO_2 samples. Our study aimed to apply two simple and cheap methods to obtain bulk materials with enhanced properties for photocatalysis, as we observed that there is a considerable scarcity of available literature on these topics.

The incipient wet impregnation (IWI) method has been previously reported as a convenient strategy for catalyst doping with various transition metals, but it has not been much considered as a valuable strategy for noble metal loading. IWI has been reported as an interesting technique for the preparation of supported catalysts due to its simplicity and the good dispersion of the dopant solution inside the internal porosity of a solid support, thus obtaining doped catalysts with very small dopant grains (even nanoparticles) well dispersed on the support.

These small areas, where the junction between the support and the doping metal occurs, provide a high number of sites with slightly different alignments of the electrons energy levels [30], leading to stabilization of the electron–hole separation and generation enhancement of active radicals with photocatalytic effects [31]. Furthermore, no noble metal loss during the photo-reactions was reported [32]. Moreover, this method has an economic and green catalyst preparation fingerprint, as there is no waste during the procedure.

The ultrasound-assisted impregnation method is a technique based on the acoustic cavitation phenomenon using ultrasonic waves. An important effect of the ultrasonication is the high dispersion of the agglomerated particles from powders dispersed in liquid media. Thus, the particles separated from each other are well exposed to the dopant from the solution, and its immobilization on the whole solid is facilitated [33]. By using this procedure, the solid is contacted with a solution volume much higher than in the IWI method. However, the uniform distribution of the dopant on the support is expected, since its dispersion in the liquid is high, and the use of volatile solvents for the procedure allows the ultrasonication to occur since the evaporation of most of the liquid is observed [34].

The fact that incipient wet impregnation and ultrasound-assisted deposition of noble metals are not often mentioned as doping procedures in the literature motivated us to apply these procedures for the improvement of a commercial titania. We chose in this respect a pure anatase product and focused our attention on its doping by using gold and palladium salts and applying the fore-mentioned techniques. Their structural characterization was performed by powder X-ray diffraction (XRD), scanning electron microscopy (SEM), Energy Dispersive X-ray Analysis (EDAX) of the surface species and ultraviolet-diffuse reflectance spectroscopy (UV-Vis/DR) to calculate the band gap values.

Then, after proving that the doping induced changes in the morphology of the solids and band gap values, their efficiency as photocatalysts with high activity towards an enhanced degradation of persistent organic water pollutants was compared. The photocatalytic activity was investigated with regard to the degradation of 2,4-dinitrophenol (2,4 DNP) as target molecule under UV-A irradiation conditions. This organic compound is a phenol derivative, well known for its carcinogenic potential and widely used as a precursor for dyes and pesticides. Being a very toxic compound with low biodegradability and hardly transformed during the conventional wastewater treatment, 2,4 DNP is often use as a test compound for the investigation of the photocatalytic activity of new synthesized

semiconductive solids [4]. The photocatalytic activity of the doped catalysts is expected to largely depend on the synthesis method and on the species of the noble metal. An enhanced elimination of 2,4 DNP was observed in the case of the TiO_2-Pd system obtained by the IWI method.

Afterwards, the photocatalytic activity of the best doped catalyst was also evaluated for the degradation of rhodamine 6 G (R6G) to determine its efficiency over an organic water pollutant with a completely different chemical structure, because this factor is recognized to affect the catalyst photoactivity. R6G is a fluorescent dye with a xanthene structure, and it is very stable in aqueous solutions. It is mainly used in the textile industry as a dyestuff, in medicine as an analogue in the P-glycoprotein (Pgp) efflux assays, as a leukocyte marker to study the interaction between leukocytes and the vascular endothelium, in Enzyme-linked immunosorbent assay—ELISA biochemical analysis and in biotechnology applications for fluorescence microscopy [35–37]. This complex molecule has considerable stability in aqueous solutions, and while its fluorescent pink color makes it easy to see even with the naked eye at concentrations as low as 1 ppm, it also makes it undesirable in the environment; thus, it is recommended as a probe molecule for the investigation of new photocatalysts. Excellent investigations regarding this dye decomposition mechanism by photocatalytic degradation are available in the literature [38,39].

With the aims of delivering a material superior to the initial TiO_2 (Across) after doping and running a process with energy consumption as low as possible, calculations of the electric energy per order were carried out to classify the photocatalysts also from this point of view.

The results of this study reveal that doping with palladium gave better results in terms of photocatalytic activity and energy consumption than both the raw material and gold-doped material for both 2,4 DNP and R6G degradation.

2. Materials and Methods

2.1. Chemicals

The commercial TiO_2 (anatase >98%) used in this work was purchased from Across Organics (Across Organics, Vienna, Austria). Palladium chloride ($PdCl_2$) and gold (I) chloride (AuCl), used as precursors for Pd and Au, were acquired from Sigma-Aldrich (Sigma-Aldrich, St. Louis, MO, USA). Hydrochloric acid (technical grade, 37%) and absolute ethanol (EtOH) were purchased from Silal Trading SRL (Silal Trading SRL, Bucharest, Romania) and Sigma-Aldrich, respectively. 2,4 DNP and R6G of analytical grade were provided by Sigma-Aldrich. All reagents were used without further purification. The 2,4 DNP and R6G working solutions were prepared by diluting stock solutions in distilled water.

2.2. Preparation of Doped TiO_2

TiO_2-Au and TiO_2-Pd were obtained by using the ultrasound method (US) (device Sonics VCX-750 Vibra Cell Ultra Sonic Processor (Sonics & Materials, Inc., Newtown, PA, USA), using pulse/pause cycles of 2/2 s) and by incipient wet impregnation (IWI). The doping degree was of 1% metal (by weight). The dopant precursors were prepared by dissolving $PdCl_2$ and AuCl in concentrated HCl using acid-to-salt ratios close to those giving saturated solutions. The samples were denoted as TiO_2-Pd/US, TiO_2-Au/US, TiO_2-Pd/IWI and TiO_2-Au/IWI.

When the US procedure was employed, 4 g of TiO_2 was mixed with 50 mL of EtOH, and the suspension was subjected to ultrasonication for 1.5 h at room temperature. Subsequently, the volume of the dopant solution corresponding to the desired doping extent was added. The same ultrasonication procedure was continued for one more hour, and then the mixture was dried at 100 °C overnight for the total evaporation of the ethanol.

For the doping procedure using the IWI technique, the initial TiO_2 sample (4 g) was dehydrated at 200 °C for two hours in a crucible introduced in an oven. Afterwards, the dopant solution prepared by diluting the corresponding dopant hydrochloric solution with

ethanol to reach a volume of 4 mL was suddenly poured on the hot solid, and the crucible was immediately covered with a cap.

All doped samples, as well as a pure TiO_2 sample, were calcined in a furnace at 600 °C at a heating rate of 2°/min for 4 h to decompose the initial salts and obtain the noble metal dispersed on TiO_2. Figure 1 summarizes the main steps of both of the methods used for the synthesis of catalysts.

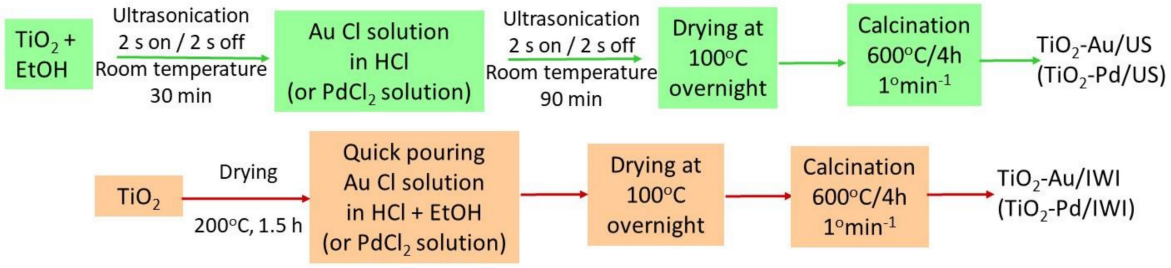


Figure 1. Flow chart of the main steps for the protocols used in this study for catalyst preparation.

2.3. Characterization

The XRD patterns were obtained on a Shimadzu D6000 device (Shimadzu Corporation, Tokyo, Japan) (2 theta range 5–80°) using CuKα radiation (λ = 1.5406 Å). The SEM images and EDAX composition measurement were obtained on a JEOL JSM 7100 F EDS EBSD Oxford microscope (JEOL JSM-7100, Jeol Ltd., Tokyo, Japan). The pure nitrogen adsorption measurements at 77 K (by submerging the sample cell in liquid nitrogen), performed on a Nova 2200 apparatus (Quantachrome Instruments, Graz, Austria), allowed the determination of the specific surface area using the BET (Brunauer-Emmett-Teller) equation. The UV–DR spectra on solid samples were traced on a Shimadzu 1700 device, preparing the sample with MgO as blank and dilution solid material.

2.4. Photocatalytic Tests

The photocatalytic activity of the synthesized solids was investigated in a glass cylindrical reactor with a total volume of about 500 mL and with internal irradiation using an Osram UV-A lamp of 9W (OSRAM GmbH, Garching, Germany) (emitting in the range of 350–400 nm with a maximum at 370 nm), hosted in a central quartz tube, using a solution with a volume of 250 mL for each test. These photocatalytic reactions were performed under magnetic stirring at room temperature and at the native pH of the solutions, using 2,4 DNP and R6G as test molecules. Stock solutions of 300 ppm were prepared from precisely weighted amounts of 2,4 DNP and R6G in volumetric flasks of 500 mL. The working solutions were prepared by properly diluting the stocks in volumetric flasks of 250 mL with distilled water. Prior to irradiation, the test solution mixed with 1 g/L of the photocatalyst was stirred in the dark to establish the adsorption-desorption equilibrium; then, the UV lamp was turned on. Samples were withdrawn at established time intervals from the reactor and filtered through a 0.45 μm syringe filter to retain the solid. The solution concentrations were measured by spectrophotometry.

2.5. Analytical Determination

The residual concentration of the pollutant was measured by spectrophotometry, using a Shimadzu UV-1700 spectrophotometer. The absorbance values were recorded at 360 nm for 2,4 DNP and at 526 nm for R6G, the corresponding absorption wavelength maxima for the analyzed molecules. For quantification purposes, Lambert-Beer law was considered. The calibration curves for each target molecule were calculated within the linear ranges of 0–15 mg/L (for 2,4-DNP) and 0–10 mg/L (for R6G) with high correlation coefficients of 0.997 and 0.994, respectively. If necessary, samples dilutions in distilled water were made before spectrophotometric analysis.

Degradation efficiency was calculated with the following equation:

$$D,\ \% = \frac{C_0 - C_t}{C_0} \cdot 100 \quad (1)$$

where C_0 is the initial concentration of the solution before the photocatalytic reaction, and C_t is the solution concentration at time t of irradiation.

3. Results and Discussions

3.1. Material Characterization

The TiO_2 parent material, after calcination at 600 °C, consisted of pure anatase, as the XRD pattern shows (Figure 2). The main peaks in the powder XRD patterns indicate the presence of the characteristic planes for anatase TiO_2: (101), (004), (200), (105), (211), (204) and (116) corresponding to maxima at 2θ = 25.4°, 37.8°, 48.1°, 53.9°, 55.1°, 62.7° and 68.8°, respectively [40]. The XRD pattern indicates a highly crystalline material, with excellent anatase phase purity. The XRD patterns of the doped samples, TiO_2-Au/IWI and TiO_2-Pd/IWI, have very similar shapes, showing the presence of low intensity maxima assigned to the (111) and (200) planes of Pd metal nanoparticles at 39.8° and 49.3° [41–43], respectively, and to the (111) plane of Au nanoparticles at 33.9° [44,45].

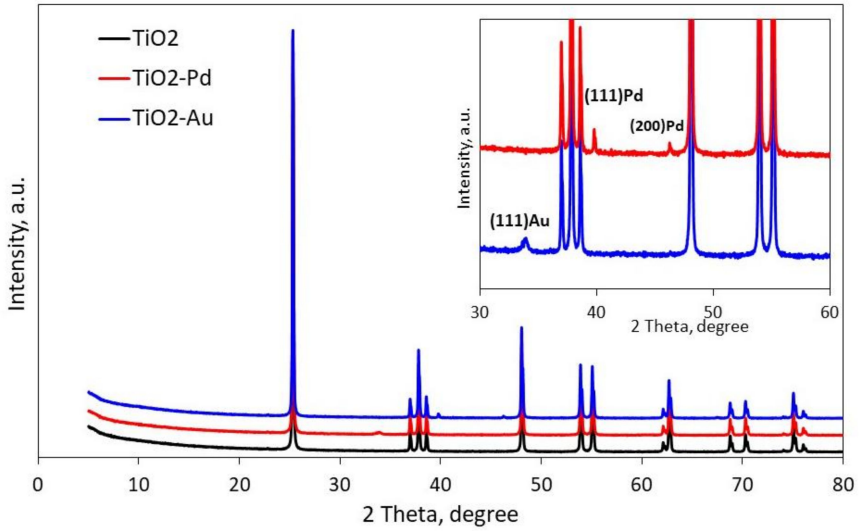


Figure 2. XRD pattern of TiO_2 support, TiO_2-Pd/incipient wet impregnation (IWI) and TiO_2-Au/IWI, calcined at 600 °C.

The position and width of the most intense peak corresponding to the (101) plane of TiO_2 were used to calculate the size of the particles using the Debye–Scherrer relation:

$$D_{cryst} = \frac{0.94\ \lambda}{(h_{1/2}\ cos\ \theta hkl)} \quad (2)$$

where $h_{1/2}$ is the width at the half-peak height.

The values of the particle size calculated by this method for our samples were 55.66 nm for genuine TiO_2, 55.98 nm for TiO_2-Pd/IWI and 55.83 nm for TiO_2-Au/IWI.

The values of the specific surfaces of the samples were 10.35 m^2/g for genuine TiO_2, 11.57 m^2/g for TiO_2-Pd/IWI, 11.04 m^2/g for TiO_2-Pd/US, 10.1 m^2/g for TiO_2-Au/IWI and 9.95 m^2/g for TiO_2-Au/US.

The SEM images (Figure 3) show that the morphology of the doped samples is very similar, regardless of the species of the noble metal. For the images on the left side, the detection is based on the capture of the secondary electrons issued during the sample bombardment with incident electrons (SEI), while the images on the right are obtained

from the capture of the retro-diffused electrons, providing a specific contrast according to the sample composition (the sample with the presence of gold provides a lighter image than the sample doped with palladium, as it is a better electronic conductor).

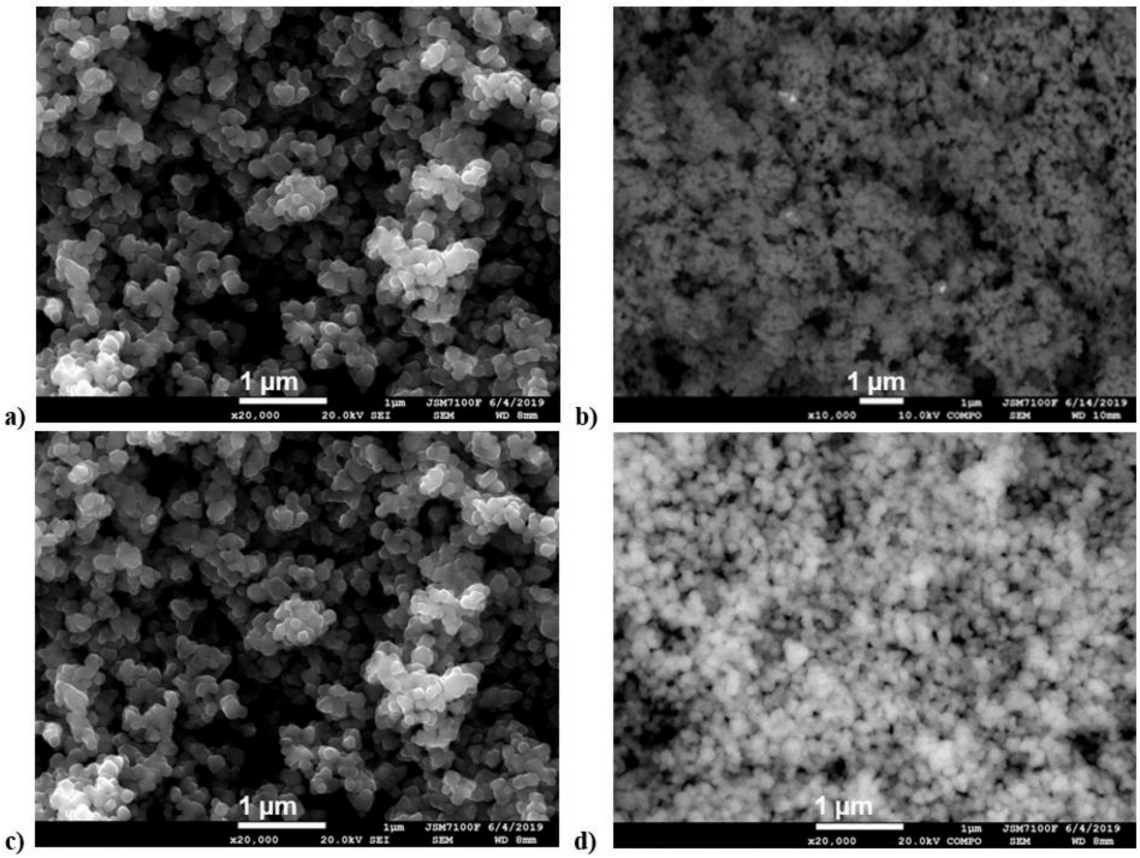


Figure 3. SEM micrographs: (**a**,**b**) of TiO_2-Pd/IWI) and (**c**,**d**) TiO_2-Au/IWI.

The noble metal mapping indeed indicates the uniform spread-out of the dopant on the support surface.

The surface composition of the TiO_2-Pd/IWI sample was highlighted by the elemental mapping (EDX) connected to SEM analysis. The images (Figure 4) indicate the presence of a small amount of Pd grains on the surface (appearing as bright spots). Furthermore, the presence of Pd nanoparticles on the surface is proved by the values of the Pd/Ti ratio measured on a surface area without Pd grains (spots 1,2 and 3 in Figure 4a).

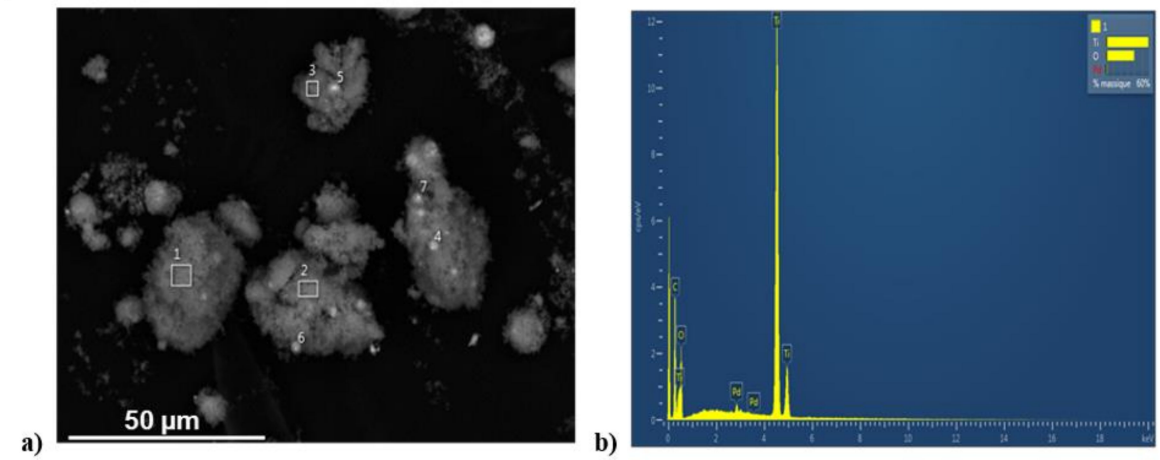


Figure 4. Elemental mapping by EDAX for the TiO_2-Pd/IWI sample: (**a**) overall aspect, (**b**) average elemental composition on the selected areas.

The analysis shows that the Pd/Ti ratio is 1.28%, which is higher than the amount introduced in the preparation (1%), indicating that the diffusion of Pd inside the porous structure of TiO_2 is quite poor: a big proportion of the Pd used in the preparation remains on the outer surface of TiO_2, where the EDAX analysis allows their detection.

The semi-conductive properties of the samples were analyzed by UV-DR spectroscopy, allowing the calculation of the band gap either by the extrapolation of the linear portion of the UV-DR curve or, even better, by tracing the Tauc plots (Figure 5) [46,47].

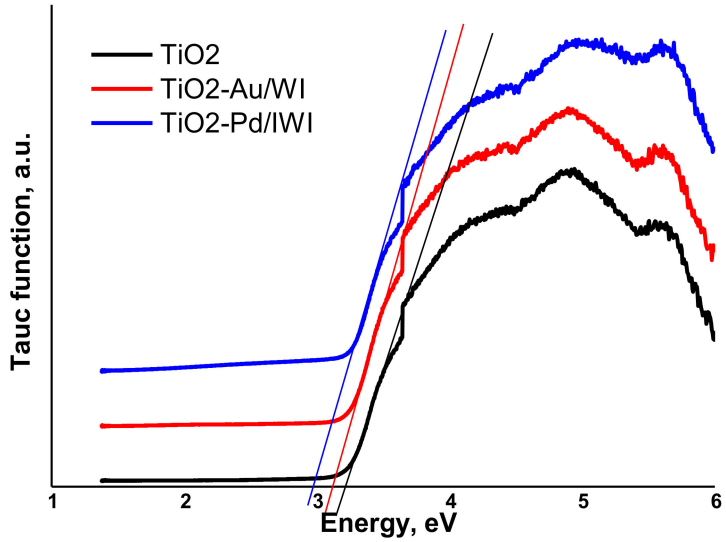


Figure 5. Tauc plots for the TiO_2-derived samples prepared by the IWI method.

The method supposes tracing the graphical dependence between the energy ($h \times \nu$) versus Tauc function $(\alpha \times h \times \upsilon)^2$ and helps to obtain the value of the band gap by the extrapolation of the linear portion of the curve since it crosses the *x*-axis; the value in the crossing point gives the band gap energy in eV.

The values of the band gaps for the samples are 3.2 eV (TiO_2), 3.08 (TiO_2-Au/IWI) and 2.98 eV (TiO_2-Pd/IWI). The doping procedure slightly decreases the band gap, potentially improving the photocatalytic performance of the solid. The band gap values for the samples prepared by the US method did not produce band gap changes with regard to initial TiO_2.

3.2. Effect of the Method Used for Catalyst Synthesis on Its Photocatalytic Performance

Numerous studies regarding the photocatalytic properties of TiO_2 indicate that the fast recombination rate of the Photogenerated e^-/h^+ pair is a major drawback. A promising strategy to overcome this limitation is noble metal doping [48]. Indeed, the use of noble metals (such as Pt, Pd, Ag and Au) as dopants represents a valuable option for the stabilization of TiO_2 due to their high Schottky barriers, avoiding the recombination of e^-/h^+ pairs or promoting the interfacial charge transfer processes [49]. According to this paper, doping with noble metals causes not only an enhancement of photocatalytic efficiency, but also an easier recovery of the metal from the solution and a reduction of the energy consumption and surface corrosion, as well as modifications of the semiconductor properties (mechanical, optical, magnetic and electronic) [49]. As previously stated, different methods were employed in the literature for noble metal doping of TiO_2, indicating their versatility in relation to photocatalyst performance.

In this context, the impact of the method used for TiO_2 doping on its photocatalytic activity was first investigated. Two methods, namely, ultrasound-assisted impregnation and incipient wet impregnation, were considered in this work, and the photocatalytic activity of the as-prepared gold-doped TiO_2 (TiO_2-Au) catalysts was studied in the degradation of 2,4 DNP (as model reaction) in order to determine the optimal doping method. The present preliminary study was performed under UV-A irradiation conditions in model

solution (distilled water) after a pre-equilibration period of 30 min. Preliminary blank adsorption–desorption tests were carried out in the dark in the presence of catalyst for 10 h. For illustration purposes only, the data corresponding to a contact time period of 120 min are presented in Figure 6. As shown in this figure, for 2,4-DNP the adsorption equilibrium is obtained in both cases within a contact time of 30 min, and less than 10% of pollutant elimination by immobilization on the solid by adsorption was observed under these conditions. In addition, photolysis assays were performed under UV-A irradiation without a catalyst, and only very slight degradation (about 2%) of the target molecule was observed. According to the results shown in Figure 6, both UV-A and the catalyst are necessary to enhance the photocatalytic reaction. Moreover, these results show that the method used in the photocatalyst preparation influences its photocatalytic activity. In the case of the catalyst doped by the IWI method, a higher elimination yield (50%) was observed after 120 min of irradiation, while only 37% was removed with that obtained by the US method.

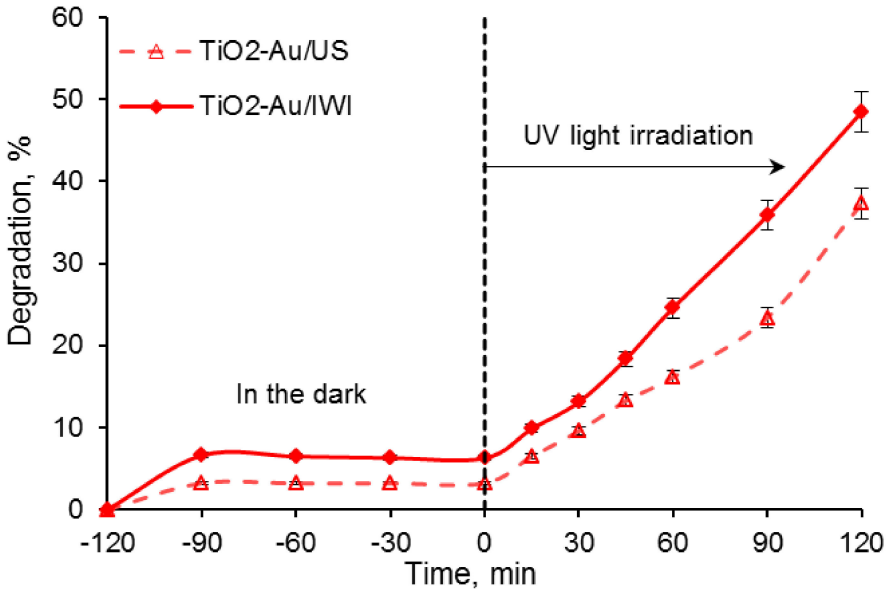


Figure 6. 2,4 dinitrophenol (2,4 DNP) degradation (20 mg/L) in the presence of the TiO_2-Au (1 g/L) catalysts, obtained by US and IWI methods.

Such behavior is due to the fact that the incipient wet impregnation method, by occurring at a high rate of contact between the support and the dopant, prevents the dopant penetration by solution diffusion into the bulk of TiO_2 and, thus, creates double phase regions on the outer surface, in which the electron–hole pair recombination rate is decreased by the refuge of the electron from the conduction band of one phase on the conduction phase of the other phase. This phenomenon is widely documented in the literature [5,7,43] and occurs on the portion of the surface accessible for the irradiation and adsorption, where the adsorbed pollutant easily interacts with the active oxidizer radicals issued from the interaction between the water molecules and promoted electrons, thus enhancing the photocatalytic performance of the doped catalyst. Indeed, Zhou et al. (2020) [50] reported that the redox reactions occurring on the catalyst surface complete the charge carrier recombination, maintaining the photocatalytic activity.

The overall photocatalytic activity of TiO_2-Au/IWI was highlighted by the UV-Vis spectra recorded at different irradiation times between 0–120 min in the range 200–800 nm (Figure 7). The maxima from the UV range of the spectra at about 227 nm are due to the nitrate group, and their intensities remain almost constant. This is an indication that the nitrate groups from the solution remain unchanged, while the aromatic portion gradually disappears: the wide peak situated between 240–210 nm becomes asymmetrical

and narrower as the reaction advances (inset Figure 7). A constant and significant decrease in the characteristic absorbance maximum at 360 nm, as well as in the shoulder from 400 nm, occurs overs time, indicating the high degradation efficiency of the target molecule in the photocatalytic system. This fact suggests that the carbon-based part of 2,4 DNP is readily mineralized to carbon dioxide and water and is not only splinted in smaller fragments, as reported earlier [51].

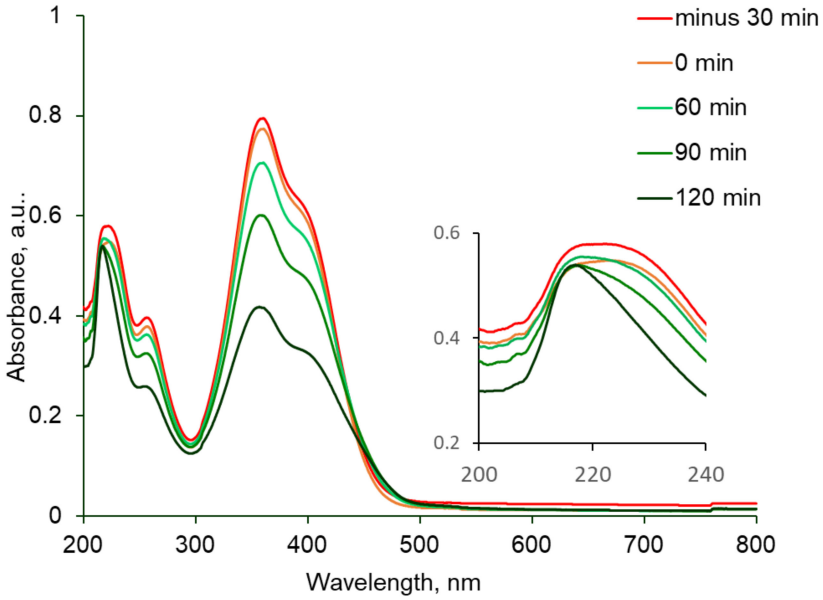


Figure 7. Temporal changes in UV-Vis absorption spectra for 2,4 DNP measured at the end of the adsorption reaction and during the photodegradation (20 mg/L) in aqueous solution in the presence of TiO_2-Au/IWI (1 g/L).

Data of several studies indicate that the ultrasound-assisted TiO_2 synthesis allows for the obtention f materials with high photocatalytic activity [52,53]. In our study, however, the results illustrate that the IWI technique provides better results than the US method. This statement is in line with other references indicating the better efficiency when IWI was used for TiO_2 doping with the aim of obtaining active solids for the photocatalytic degradation of different organic pollutants [54–57].

On the basis of these preliminary results, the IWI method was employed for the synthesis of noble metal-doped TiO_2 used in the further experiments.

3.3. Investigation of the Photocatalytic Activity of Palladium- and Gold-Doped Titania Nanoparticles Synthesized by the IWI Method

In this work, TiO_2 was doped with noble metals such as gold and palladium by the incipient wet impregnation procedure, and their photocatalytic performance was investigated under UV-A irradiation in order to define the better-performing catalyst. The degradation experiments were conducted with 2,4 DNP as target molecule for an initial concentration of 20 mg/L at a catalyst load of 1 g/L. For comparison purposes, experiments using the corresponding undoped catalyst were also conducted under similar operating conditions. Figure 8 shows the evolution in time of the 2,4 DNP degradation using Au- and Pd-doped titanium dioxide in comparison with pure TiO_2, as well as the obtained results for the dark adsorption experiments. Accordingly, it was found that the extent of the 2,4 DNP adsorbed at the surface of TiO_2-Pd/IWI (10%) is slightly higher when compared to TiO_2-Au/IWI and the undoped material. The results from the dark tests also confirm that adsorption–desorption equilibrium is reached after a contact time of 30 min. In addition, it was observed that TiO_2 doped with Pd exhibits the highest photocatalytic activity, performing a 2,4 DNP elimination yield of 70% after 120 min of irradiation. On the contrary, gold doping reduces the photoactivity compared with undoped TiO_2, decreasing

its activity by more than 10%; the TiO_2-Au/IWI catalyst shows only 50% of elimination during the same reaction time. Such behavior has been previously observed in some earlier studies, implying the use of Au-doped TiO_2 for the photodegradation of other organic pollutants [58,59]. The decrease in the photocatalytic activity observed in our study for TiO_2-Au/IWI may be due to the preparation method associated with the modification of the TiO_2 surface having a harmful effect on the photocatalytic activity because of the shadowing effect of the dopant of the TiO_2 active sites [16].

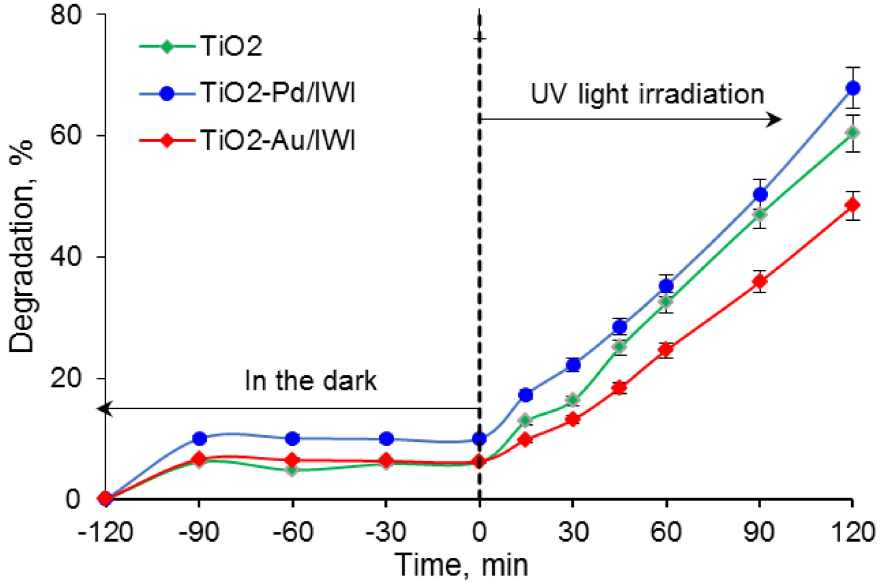


Figure 8. 2,4 DNP degradation in aqueous solution in the presence of the TiO_2-Acros, TiO_2-Pd and TiO_2-Au catalysts obtained by the IWI method.

The beneficial effect of Pd as a dopant on the photocatalytic efficiency was reported for the degradation of different water pollutants. Various studies confirmed that Pd ions can improve the photocatalytic activity by enhancing the generation of charge carriers and suppress the e^-/h^+ recombination [60,61]. Thus, the formation of reactive species responsible for the degradation of organic pollutants increases, resulting in a higher photocatalytic activity [58,62,63].

It should be noted that noble metals such as Pt or Au are quite expensive. Thus, TiO_2 metallization with cheaper metals such as palladium has a practical application potential, because it is cheaper and a lot more abundant (50 times) on Earth than platinum [16]. Combining the good results concerning the strong photocatalytic activity with the acceptable cost of palladium and its abundance, the preliminary data obtained in our study are very promising. On the other hand, one of the most relevant factors that illustrate process efficiency is economic performance. According to literature data, the electric energy spent for the advanced oxidation processes (AOP) processes is one of the main operating costs [2,63]. Given the fact that heterogeneous photocatalysis is an energy intensive process, the calculation of the electrical consumption is of practical interest. For a low initial pollutant concentration, as is the case of our study, a useful parameter that could be considered is the electrical energy per order (E_{E0}). In their earlier studies, Cardoso et al. (2016) [2] and Urkude et al. (2014) [64] defined E_{E0} as the electrical energy expressed by the number of kilowatt hours (kWh) consumed to reduce the pollutant concentration by 1 order of magnitude per unit volume of contaminated water.

For a batch reactor E_{E0} (kWh/m^3/order), the following equation can be obtained:

$$E_{E0} = \frac{P \cdot t \cdot 100}{V \cdot 60 \cdot \log\left(\frac{C_i}{C_f}\right)} \quad (3)$$

where P is the rated power (kW) of the UV-A lamp used for the photocatalytic oxidation reaction, t is the irradiation time (min), V is the working volume of the reactor (L), and C_i and C_f are the initial and the final concentration of the pollutant, respectively.

As stated above, the interest in noble metal doping is not only to extend catalyst photoactivity, but also to reduce energy consumption required for the photocatalytic reaction. Hence, for this reason, we focused our attention on the evaluation of this parameter with regard to the considered catalysts. Such an evaluation will give us more insights regarding their practical interest. Indeed, the economical factor is often dominant for the implementation of future processes. Thus, the E_{E0} values for the degradation of 2,4 DNP under UV irradiation using TiO_2-Acros, TiO_2-Au/IWI and TiO_2-Pd/IWI were calculated for a reaction time of 120 min, accordingly to Equation (3). The E_{E0} values were determined for the considered operating conditions by using these three photocatalysts, which are displayed in Figure 9.

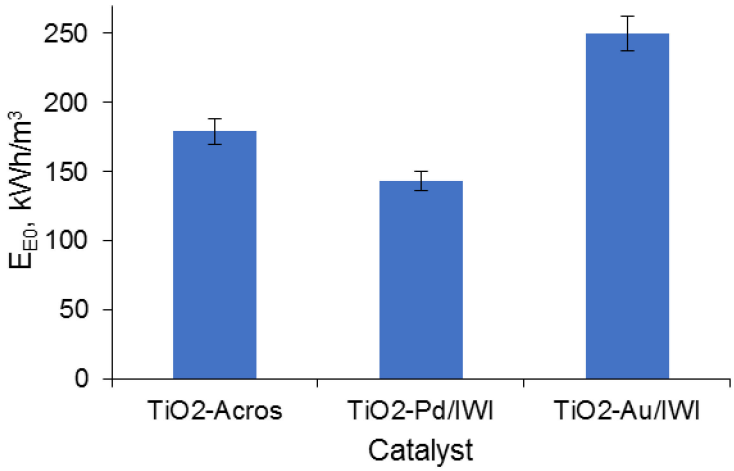


Figure 9. Energy consumption for the obtained catalyst.

An significant decrease in energy consumption was achieved using the TiO_2-Pd/IWI catalyst due to the doping in comparison with the undoped material. When calculating the ratios between the energy consumption, the value for the TiO_2-Pd/IWI sample is lower by a factor of 1.75 when compared to TiO_2-Au/IWI and by 1.25 when compared to the undoped TiO_2. These results demonstrate that the TiO_2-Pd system obtained by incipient wet impregnation represents an interesting option for the elimination of this organic pollutant due to both its efficiency in photocatalytic degradation and the substantial reduction of the energy requirement.

3.4. Evaluation of TiO_2 and TiO_2-Pd/IWI Nanoparticle Efficiency on the Elimination of 2,4 DNP and R6G

The photocatalytic activity of a catalyst strongly depends on the chemical structure of the considered pollutant [29,65]. In this context, in order to study and compare the ability of undoped TiO_2 and TiO_2-Pd/IWI to decompose different organic pollutants, additional photocatalytic tests using R6G were conducted under the same experimental conditions (initial pollutant concentration of 20 mg/L, catalyst loading of 1 g/L and use of UV-A irradiation). 2,4 DNP is a model molecule with two nitro groups and one aromatic ring. It is considered a precursor for pesticides and is often used for testing the photocatalytic potential of a solid due to its chemical stability and noticeable intrinsic toxicity, therefore being filed as a refractory compound with respect to its removal from diluted aqueous solutions. R6G is an xanthene derivative with a molar mass of 442.5. It contains two amino groups, one of them coordinated by HCl, and an aromatic ring bonded to an ester group (Figure 10 inset), has remarkable stability in aqueous solutions, and generates high color intensity, even at concentrations as low as 1 ppm [66].

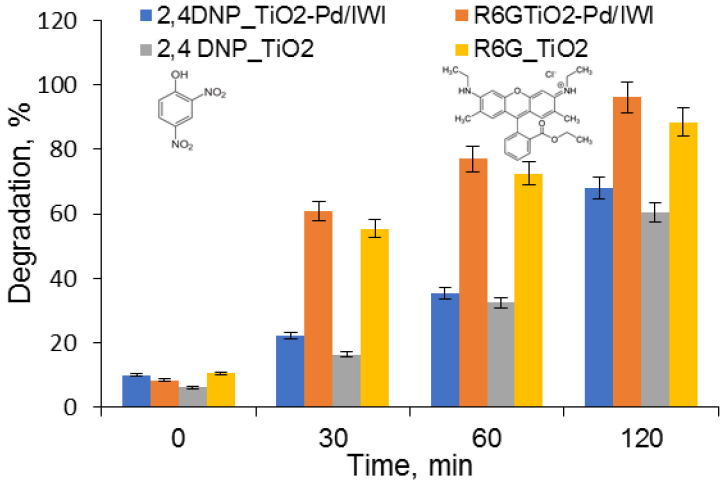


Figure 10. 2,4 DNP and rhodamine 6G (R6G) degradation in the presence of TiO_2-Pd/IWI and TiO_2. Experimental conditions: photocatalyst dose = 1g/L; pollutant = 20 mg/L.

The evolution of R6G removal by photocatalysis for the two organic species on the two catalyst samples is depicted in Figure 10 for selected reaction time durations from 0 to 120 min. The results reveal that there are substantial differences between the two catalysts on one part, and on the degraded species on another. The highest removal yield for this series of experiments was achieved for R6G on the TiO_2-Pd/IWI sample (96% decolorization degree) at 120 min of irradiation, while on the genuine TiO_2, the decolorization reached about 88% in this time duration. It indicated a more active catalyst after the doping procedure. Regarding the degradation of 2,4 DNP, the decomposition of this compound proved to be more difficult, both on Pd-doped and genuine TiO_2: the maximum decomposition yield was around 67% on TiO_2-Pd/IWI and 60% on the genuine TiO_2. The superiority of the photocatalytic activity was exhibited on the whole explored time duration. Therefore, a series of catalyst reuse was performed on the TiO_2-Pd/IWI sample. Blank experiments carried out on TiO_2-Pd/IWI in the dark with R6G, under similar experimental conditions excluding the irradiation, indicated an elimination degree of about 8%.

It must be pointed out that the catalyst investigated here prepared by using the incipient impregnation method displays good photocatalytic reactivity for both of the organic pollutants. The evolution of the decomposition yield of these two organic species in time suggests their similar behaviors in the sense of a substantial increase in the decomposed amount of the test molecule every 30 min, despite their huge differences in chemical composition and structure: R6G is readily soluble in water and its aqueous solution of 20 ppm has a native pH of 4.24, while 2,4 DNP is soluble in water only after adding diluted NaOH to induce molecule ionization.

Furthermore, the evolution of photocatalytic efficiency of TiO_2-Pd/IWI and TiO_2 over time was evaluated by the calculation of the degradation kinetics of 2,4 DNP and R6G by applying the pseudo-first-order kinetic model using the following equation:

$$-\ln\left(\frac{C_t}{C_0}\right) = K_{\text{app}}t \quad (4)$$

where C_0 is the initial concentration of the pollutant, C_t is the concentration at time t, and K_{aap} and t are the apparent reaction rate constant and the irradiation time, respectively.

According to Equation (4), K_{app} can be determined as the slope of the plot of $-\ln(C/C_0)$ versus the reaction time (Figure 11).

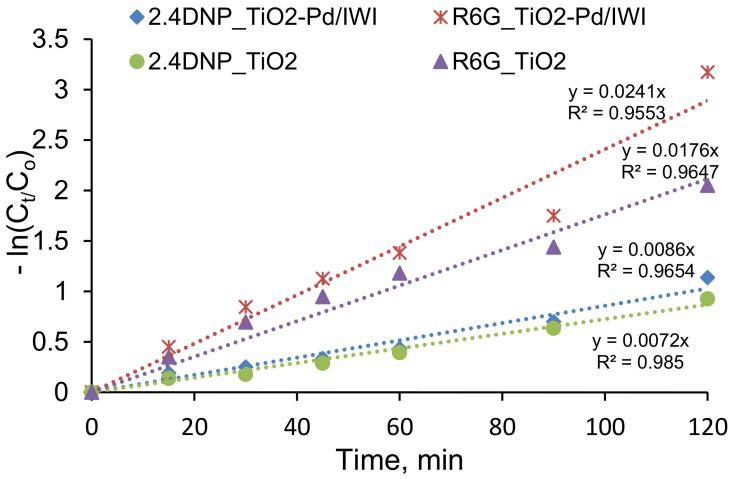


Figure 11. Reaction kinetics profiles for the degradation of 2,4 DNP and R6G in the presence of TiO_2-Pd/IWI and TiO_2. Experimental conditions: photocatalyst dose = 1g/L; pollutant = 20 mg/L.

The good plot linearity demonstrates that the photocatalytic kinetics for both organic test species follow the pseudo-first-order kinetic model. Furthermore, according to the data in Figure 11, the high values of the correlation coefficients ($R^2 > 0.93$) confirm the validity of the pseudo-first order model.

The calculated values for K_{app} were of 8.6×10^{-3} 1/min (2,4 DNP) and 2.41×10^{-2} 1/min (R6G) on the TiO_2-Pd/IWI sample and 7.2×10^{-3} 1/min (2,4 DNP) and 1.76×10^{-3} 1/min (R6G) on undoped TiO_2. They indicate that the TiO_2-Pd/IWI photocatalyst exhibits a faster and slightly higher degradation activity for both R6G and 2,4 DNP than the undoped sample, and that R6G is decomposed to a higher extent by both solids. These findings indicate that the molecule breakage of R6G is easier in the sense of chromophore group distruction; the spectrophotometric analysis shows only the color disapearance and does not provide indications regarding the mineralization of the organic species.

In summary, it is important to note that these results indicate strong evidence regarding the ability of TiO_2-Pd/IWI to degrade organic pollutants from water and, therefore, to be an efficient catalyst that can be successfully used in heterogeneous photocatalytic processes.

3.5. Investigation of Catalyst Recyclability

Another aspect examined in this study was the potential of catalyst recyclability. This evaluation represents a critical issue for future practical application of a photocatalyst in an advance oxidation process. For this reason, four photocatalytic consecutive runs were carried out in the presence of fresh prepared solutions of 2,4 DNP (initial concentration of 20 mg/L) and a catalyst of 1 g/L. After each experiment, the aqueous suspension was filtered in order to separate the TiO_2-Pd/IWI catalyst. Before its use in a new photocatalytic experiment, the collected material was washed several times with ultrapure water and afterwards dried in an oven at 100 °C for 24 h.

It should be noted that each cycle was performed using the same experimental procedure, and the pollutant elimination efficiency was monitored for a reaction duration of 120 min. According to Figure 12, the photocatalytic activity of the synthesized material was mostly unchanged. Only a slight decrease in removal of 2,4 DNP of about 7.6% was observed at the end of the fourth photocatalytic run. This result confirms the reuse potential of the TiO_2-Pd/IWI catalyst within its photocatalytic successive operation. The slight drop recorded for the elimination of the target molecule can be due to a possible catalyst loss within the filtration or rinsing steps, or it can be a result of the absorption of reaction intermediates at the catalyst surface or in its pore channels [61]. Similar results were previously reported in terms of photocatalytic stability for other catalysts or for noble metal-doped titanium dioxide for the degradation of other organic pollutants [23,62,67,68].

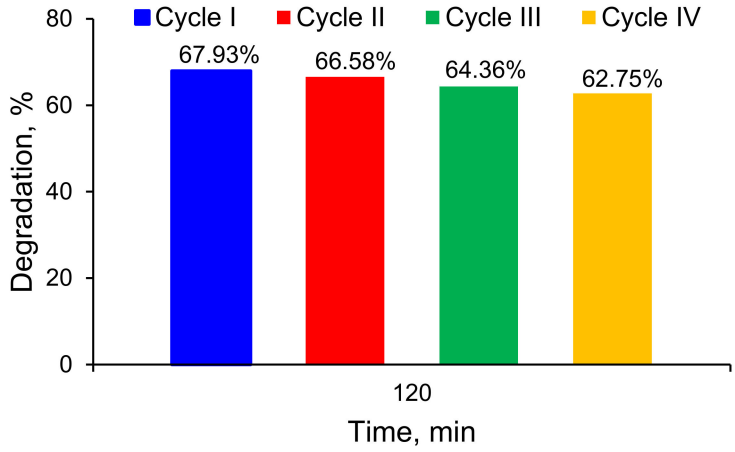


Figure 12. Variation of 2,4 DNP photodegradation efficiency within four consecutive reaction cycles on TiO_2-Pd/IWI.

The results obtained in our study clearly demonstrate the good physico-chemical stability of the used material, providing clear evidence regarding its promising potential for future practical photocatalytic applications.

4. Conclusions

The noble metal doping of TiO_2 is a versatile method for improving the photocatalytic activity, especially when the dopant is accessible and has a reasonable price. In the present study, the doping of a commercial titania (Across Chemicals, Vienna, Austria) containing anatase phase has only been performed with gold and palladium, by either applying the impregnation under ultrasound treatment in alcoholic suspension (US) or by employing the incipient wet impregnation technique (IWI).

The materials were characterized by XRD, SEM, EDAX, BET adsorption of pure nitrogen and UV–DR spectroscopy and revealed the formation of small dopant particles on the support.

Preliminary tests of 2,4 DNP degradation by photocatalysis highlighted that the IWI technique provides better photo-active materials than those obtained by the US method. The energy consumption for the UV irradiation was calculated, and a decrease of 25% is observed in the case of TiO_2-Pd/IWI in comparison with the TiO_2 support.

The photocatalytic potential of the TiO_2 sample doped with Pd was evaluated by using two organic species, 2,4-dinitrophenol (and 2,4 DNP) and rhodamine 6G (R6G). Despite its bulk and complex molecule, R6G was degraded deeper and faster than 2,4 DNP; within 120 min of photocatalyst action under UV irradiation, 96% of elimination was found for the R6G dye. The obtained results also show that the reaction kinetics for both 2,4 DNP and R6G were well fitted to a pseudo-first model. Moreover, the obtained data clearly demonstrated the high photocatalytic stability of the synthesized TiO_2-Pd/IWI catalyst, showing good reactivity in the degradation of 2,4 DNP after a few repeated cycles of degradation/regeneration, which is very promising for a future practical application.

To conclude, the present study provides new evidence that the IWI method represents a promising option for the synthesis of palladium-doped titanium dioxide with high photocatalytic activity for the oxidation of persistent organic pollutants under UV-A irradiation conditions. Furthermore, we hope that the results reported in our study will certainly stimulate future research on the optimization of the synthesis conditions for IWI protocol in order to design optimized TiO_2-Pd systems with enhanced photocatalytic activity suitable for environmental applications.

Author Contributions: Conceptualization, L.F. and D.L.; Methodology, M.H.; Validation, A.M.S., G.C. and L.F.; Investigation, A.M.S., N.S.-D. and D.L.; Resources, L.F.; Writing—original draft preparation,

D.L.; Writing—review and editing, L.F.; Visualization, M.H.; Supervision, L.F. All authors have read and agreed to the published version of the manuscript.

Funding: This research received no external funding.

Institutional Review Board Statement: Not applicable.

Informed Consent Statement: Not applicable.

Data Availability Statement: The data presented in this study are available on request from the corresponding author.

Acknowledgments: The authors are thankful to "Gheorghe Asachi" Technical University of Iasi for funding PhD student mobility.

Conflicts of Interest: The authors declare no conflict of interest.

References

1. Favier, L.; Harja, M.; Simion, A.I.; Rusu, L.; Kadmi, Y.; Pacala, M.L.; Bouzaza, A. Advanced oxidation process for the removal of chlorinated phenols in aqueous suspensions. *J. Environ. Prot. Ecol.* **2016**, *17*, 1132–1141.
2. Cardoso, J.C.; Bessegato, G.G.; Zanoni, M.V.B. Efficiency comparison of ozonation, photolysis, photocatalysis and photoelectrocatalysis methods in real textile wastewater decolorization. *Water Res.* **2016**, *98*, 39–46. [CrossRef] [PubMed]
3. Favier, L.; Rusu, L.; Simion, A.I.; Hlihor, R.; Pacala, M.L.; Augustyniak, A. Efficient degradation of clofibric acid through a heterogeneous photocatalytic oxidation process. *Environ. Eng. Manag. J.* **2019**, *18*, 1683–1692. [CrossRef]
4. Lutic, D.; Petrovschi, D.; Ignat, M.; Crețescu, I.; Bulai, G. Mesoporous cerium-doped titania for the photocatalytic removal of persistent dyes. *Catal. Today* **2018**, *306*, 300–309. [CrossRef]
5. Ahmed, S.; Rasul, M.G.; Brown, R.; Hashib, M.A. Influence of parameters on the heterogeneous photocatalytic degradation of pesticides and phenolic contaminants in wastewater: A short review. *J. Environ. Manag.* **2011**, *92*, 311–330. [CrossRef]
6. Vrinceanu, N.; Hlihor, R.M.; Simion, A.I.; Rusu, L.; Fekete-Kertész, I.; Barka, N.; Favier, L. New Evidence of the Enhanced Elimination of a Persistent Drug Used as a Lipid Absorption Inhibitor by Advanced Oxidation with UV-A and Nanosized Catalysts. *Catalysts* **2019**, *9*, 761. [CrossRef]
7. Pelaez, M.; Nolan, N.T.; Pillai, S.C.; Seery, M.K.; Falaras, P.; Kontos, A.G.; Dunlop, P.S.M.; Hamilton, J.W.J.; Byrne, J.A.; O'Shea, K.; et al. A review on the visible light active titanium dioxide photocatalysts for environmental applications. *Appl. Catal. B Environ.* **2012**, *125*, 331–349. [CrossRef]
8. Madjene, F.; Aoudjit, L.; Igoud, S.; Lebik, H.; Boutra, B. A review: Titanium dioxide photocatalysis for water treatment. *Trans. J. Sci. Technol.* **2013**, *3*, 1857–8047.
9. Elhalil, A.; Elmoubarki, R.; Sadiq, M.; Abdennouri, M.; Kadmi, Y.; Favier, L.; Qourzal, S.; Barka, N. Enhanced photocatalytic degradation of caffeine as a model pharmaceutical pollutant by Ag-ZnO-Al_2O_3 nanocomposite. *Desalin. Water Treat.* **2017**, *94*, 254–262. [CrossRef]
10. Favier, L.; Simion, A.I.; Matei, E.; Grigoras, C.G.; Kadmi, Y.; Bouzaza, A. Photocatalytic oxidation of a hazardous phenolic compound over TiO_2 in a batch system. *Environ. Eng. Manag. J.* **2016**, *15*, 1059–1067. [CrossRef]
11. Giahi, M.; Pathania, D.; Agarwal, S.; Ali, G.A.; Chong, K.F.; Gupta, V.K. Preparation of Mg-doped TiO_2 nanoparticles for photocatalytic degradation of some organic pollutants. *Studia UBB Chem.* **2019**, *64*, 7–18. [CrossRef]
12. Favier, L.; Harja, M. TiO_2/fly ash nanocomposite for photodegradation of persistent organic pollutant. In *Handbook of Nanomaterials and Nanocomposites for Energy and Environmental Applications*; Kharissova, O., Martínez, L., Kharisov, B., Eds.; Springer International Publishing: Cham, Switzerland, 2020. [CrossRef]
13. Mansour, S.A.; Farha, A.H.; Kotkata, M.F. Sol–Gel Synthesized Co-Doped Anatase TiO_2 Nanoparticles: Structural, Optical, and Magnetic Characterization. *J. Inorg. Organomet. Polym. Mater.* **2019**, *29*, 1375–1382. [CrossRef]
14. Sachs, M.; Pastor, E.; Kafizas, A.; Durrant, J.R. Evaluation of surface state mediated charge recombination in anatase and rutile TiO_2. *J. Phys. Chem. Lett.* **2016**, *7*, 3742–3746. [CrossRef] [PubMed]
15. Harja, M.; Sescu, A.M.; Favier, L.; Lutic, D. Doping Titanium Dioxide with Palladium for Enhancing the Photocatalytic Decontamination and Mineralization of a Refractory Water Pollutant. *Rev. Chim.* **2020**, *71*, 145–152. [CrossRef]
16. Alaoui, O.T.; Herissan, A.; Le Quoc, C.; el Mehdi Zekri, M.; Sorgues, S.; Remita, H.; Colbeau-Justin, C. Elaboration, charge-carrier lifetimes and activity of Pd-TiO_2 photocatalysts obtained by gamma radiolysis. *J. Photochem. Photobiol. A* **2012**, *242*, 34–43. [CrossRef]
17. Maicu, M.; Hidalgo, M.C.; Colón, G.; Navío, J.A. Comparative study of the photodeposition of Pt, Au and Pd on pre-sulphated TiO_2 for the photocatalytic decomposition of phenol. *J. Photochem. Photobiol. A* **2011**, *217*, 275–283. [CrossRef]
18. De Castro, C.G.; Duduman, C.N.; Harja, M.; Lutic, D.; Juzsakova, T.; Cretescu, I. New TiO_2-Ag nanoparticles used for organic compounds degradation. *Environ. Eng. Manag. J.* **2019**, *18*, 1755–1763.
19. Duduman, C.N.; Harja, M.; Barrena Pérez, M.I.; de Castro, C.G.; Lutic, D.; Kotova, O.; Cretescu, I. Preparation and characterization of nanocomposite material based on TiO_2-Ag for environmental applications. *Environ. Eng. Manag. J.* **2018**, *17*, 925–936.

20. Mohammad-Salehi, H.; Hamadanian, M.; Safardoust-Hojaghan, H. Visible-Light Induced Photodegradation of Methyl Orange via Palladium Nanoparticles Anchored to Chrome and Nitrogen Doped TiO_2 Nanoparticles. *J. Inorg. Organomet. Polym. Mater.* **2019**, *29*, 1457–1465. [CrossRef]
21. Sakthivel, S.; Shankar, M.V.; Palanichamy, M.; Arabindoo, B.; Bahnemann, D.W.; Murugesan, V. Enhancement of photocatalytic activity by metal deposition: Characterization and photonic efficiency of Pt, Au and Pd deposited on TiO_2 catalyst. *Water Res.* **2004**, *38*, 3001–3008. [CrossRef]
22. Khaoulani, S.; Chaker, H.; Cadet, C.; Bychkov, E.; Cherif, L.; Bengueddach, A.; Fourmentin, S. Wastewater treatment by cyclodextrin polymers and noble metal/mesoporous TiO_2 photocatalysts. *C. R. Chim.* **2015**, *18*, 23–31. [CrossRef]
23. Wang, R.; Tang, T.; Wei, Y.; Dang, D.; Huang, K.; Chen, X.; Yin, H.; Tao, X.; Lin, Z.; Dang, Z.; et al. Photocatalytic debromination of polybrominated diphenyl ethers (PBDEs) on metal doped TiO_2 nanocomposites: Mechanisms and pathways. *Environ. Int.* **2019**, *127*, 5–12. [CrossRef] [PubMed]
24. Ribao, P.; Corredor, J.; Rivero, M.J.; Ortiz, I. Role of reactive oxygen species on the activity of noble metal-doped TiO_2 photocatalysts. *J. Hazard. Mater.* **2019**, *372*, 45–51. [CrossRef] [PubMed]
25. Gomes, J.F.; Lopes, A.; Bednarczyk, K.; Gmurek, M.; Stelmachowski, M.; Zaleska-Medynska, A.; Quinnta-Ferreira, E.; Costa, R.; Quinnta-Ferreira, R.; Martins, R.C. Effect of noble metals (Ag, Pd, Pt) loading over the efficiency of TiO_2 during photocatalytic ozonation on the toxicity of parabens. *ChemEngineering* **2018**, *2*, 4. [CrossRef]
26. Hu, C.; Tang, Y.; Jiang, Z.; Hao, Z.; Tang, H.; Wong, P.K. Characterization and photocatalytic activity of noble-metal-supported surface TiO_2/SiO_2. *Appl. Catal. A Gen.* **2003**, *253*, 389–396. [CrossRef]
27. Iliev, V.; Tomova, D.; Bilyarska, L.; Eliyas, A.; Petrov, L. Photocatalytic properties of TiO_2 modified with platinum and silver nanoparticles in the degradation of oxalic acid in aqueous solution. *Appl. Catal. B* **2006**, *63*, 266–271. [CrossRef]
28. Klein, M.; Nadolna, J.; Gołąbiewska, A.; Mazierski, P.; Klimczuk, T.; Remita, H.; Zaleska-Medynska, A. The effect of metal cluster deposition route on structure and photocatalytic activity of mono-and bimetallic nanoparticles supported on TiO_2 by radiolytic method. *Appl. Surf. Sci.* **2016**, *378*, 37–48. [CrossRef]
29. Nguyen, C.H.; Fu, C.C.; Juang, R.S. Degradation of methylene blue and methyl orange by palladium-doped TiO_2 photocatalysis for water reuse: Efficiency and degradation pathways. *J. Clean. Prod.* **2018**, *202*, 413–427. [CrossRef]
30. Delannoy, L.; El Hassan, N.; Musi, A.; Le To, N.N.; Krafft, J.M.; Louis, C. Preparation of supported gold nanoparticles by a modified incipient wetness impregnation method. *J. Phys. Chem. B* **2006**, *110*, 22471–22478. [CrossRef]
31. Yang, C.; Zhao, Z.Y. Interfacial properties and band alignment of noble-metal/anatase TiO_2 (101) hetero-structures. *Comput. Mater. Sci.* **2018**, *151*, 160–173. [CrossRef]
32. Baatzi, C.; Prüße, U. Preparation of gold catalysts for glucose oxidation by incipient wetness. *J. Catal.* **2007**, *249*, 34–40. [CrossRef]
33. Stucchi, M.; Bianchi, C.L.; Argirusis, C.; Pifferi, V.; Neppolian, B.; Cerrato, G.; Boffito, D.C. Ultrasound assisted synthesis of Ag-decorated TiO_2 active in visible light. *Ultrason. Sonochem.* **2018**, *40*, 282–288. [CrossRef] [PubMed]
34. Rahmani, F.; Haghighi, M.; Vafaeian, Y.; Estifaee, P. Hydrogen production via CO_2 reforming of methane over ZrO_2-Doped Ni/ZSM-5 nanostructured catalyst prepared by ultrasound assisted sequential impregnation method. *J. Power Sources* **2014**, *272*, 816–827. [CrossRef]
35. Rajoriya, S.; Bargole, S.; Saharan, V.K. Degradation of a cationic dye (Rhodamine 6G) using hydrodynamic cavitation coupled with other oxidative agents: Reaction mechanism and pathway. *Ultrason. Sonochem.* **2017**, *34*, 183–194. [CrossRef]
36. Sescu, A.M.; Harja, M.; Lutic, D.; Favier, L.; Ciobanu, G. Photocatalytic activity of dopped TiO_2 over organic compounds degradation. *Ann. Acad. Rom. Sci. Ser. Phys. Chem. Sci.* **2019**, *4*, 69–75.
37. Shoukat, S.; Rehman, W.; Haq, S.; Waseem, M.; Shah, A. Synthesis and characterization of zinc stannate nanostructures for the adsorption of chromium (VI) ions and photo-degradation of rhodamine 6G. *Mater. Res. Express* **2019**, *6*, 115052. [CrossRef]
38. Rasheed, T.; Bilal, M.; Iqbal, H.M.; Hu, H.; Zhang, X. Reaction mechanism and degradation pathway of rhodamine 6G by photocatalytic treatment. *Water Air Soil Pollut.* **2017**, *228*, 291. [CrossRef]
39. Georgekutty, R.; Seery, M.K.; Pillai, S.C. A highly efficient Ag-ZnO photocatalyst: Synthesis, properties, and mechanism. *J. Phys. Chem. C* **2008**, *112*, 13563–13570. [CrossRef]
40. Hanaor, D.A.; Sorrell, C.C. Review of the anatase to rutile phase transformation. *J. Mater. Sci.* **2011**, *46*, 855–874. [CrossRef]
41. Yilmaz, Ü.; Küçükbay, H.; Çelikesir, S.T.; Akkurt, M.; Büyükgüngör, O. Synthesis of novel benzimidazole salts and microwave-assisted catalytic activity of in situ generated Pd nanoparticles from a catalyst system consisting of benzimidazol salt, Pd (OAc)_2, and base in a Suzuki-Miyaura reaction. *Turk. J. Chem.* **2013**, *37*, 721–733. [CrossRef]
42. Kumar, P.R.; Vivekanandhan, S.; Misra, M.; Mohanty, A.; Satyanarayana, N. Soybean (Glycine max) leaf extract based green synthesis of palladium nanoparticles. *J. Biomater. Nanobiotechnol.* **2012**, *3*, 14–19. [CrossRef]
43. Afsari, M.; Youzbashi, A.A.; Nuranian, H.; Zahraee, S.M. Remarkable improvement of visible light photocatalytic activity of TiO_2 nanotubes doped sequentially with noble metals for removing of organic and microbial pollutants. *Mater. Res. Bull.* **2017**, *94*, 15–21. [CrossRef]
44. Ren, X.; Song, Y.; Liu, A.; Zhang, J.; Yang, P.; Zhang, J.; An, M. Experimental and theoretical studies of DMH as a complexing agent for a cyanide-free gold electroplating electrolyte. *RSC Adv.* **2015**, *5*, 64997–65004. [CrossRef]
45. Krishnamurthy, S.; Esterle, A.; Sharma, N.C.; Sahi, S.V. Yucca-derived synthesis of gold nanomaterial and their catalytic potential. *Nanoscale Res. Lett.* **2014**, *9*, 627. [CrossRef] [PubMed]

46. Suram, S.K.; Newhouse, P.F.; Gregoire, J.M. High throughput light absorber discovery, Part 1: An algorithm for automated tauc analysis. *ACS Comb. Sci.* **2016**, *18*, 673–681. [CrossRef] [PubMed]
47. Tauc, J.; Grigorovici, R.; Vancu, A. Optical Properties and Electronic Structure of Amorphous Germanium. *Phys. Status Solidi B* **1966**, *15*, 627–637. [CrossRef]
48. Gómez-Pastora, J.; Dominguez, S.; Bringas, E.; Rivero, M.J.; Ortiz, I.; Dionysiou, D.D. Review and perspectives on the use of magnetic nanophotocatalysts (MNPCs) in water treatment. *Chem. Eng. J.* **2017**, *310*, 407–427. [CrossRef]
49. Ziylan-Yavas, A.; Mizukoshi, Y.; Maeda, Y.; Ince, N.H. Supporting of pristine TiO_2 with noble metals to enhance the oxidation and mineralization of paracetamol by sonolysis and sonophotolysis. *Appl. Catal. B Environ.* **2015**, *172–173*, 7–17. [CrossRef]
50. Zhou, Y.; Ding, Q.; Wang, Y.; OuYang, X.; Liu, L.; Li, J.; Wang, B. Carrier Transfer and Capture Kinetics of the $TiO_2/Ag_2V_4O_{11}$ Photocatalyst. *Nanomaterials* **2020**, *10*, 828. [CrossRef]
51. Lutic, D.; Creţescu, I. Optimization study of rhodamine 6G removal from aqueous solutions by photocatalytic oxidation. *Rev. Chim.* **2016**, *67*, 134–138.
52. Ambati, R.; Gogate, P.R. Ultrasound assisted synthesis of iron doped TiO_2 catalyst. *Ultrason. Sonochem.* **2018**, *40*, 91–100. [CrossRef] [PubMed]
53. Deshmukh, S.P.; Kale, D.P.; Kar, S.; Shirsath, S.R.; Bhanvase, B.A.; Saharan, V.K.; Sonawane, S.H. Ultrasound assisted preparation of rGO/TiO_2 nanocomposite for effective photocatalytic degradation of methylene blue under sunlight. *Nano-Struct. Nano-Objects* **2020**, *2*, 100407. [CrossRef]
54. Van de Moortel, W.; Kamali, M.; Sniegowski, K.; Braeken, L.; Degrève, J.; Luyten, J.; Dewil, R. How Photocatalyst Dosage and Ultrasound Application Influence the Photocatalytic Degradation Rate of Phenol in Water: Elucidating the Mechanisms Behind. *Water* **2020**, *12*, 1672. [CrossRef]
55. Bobirică, C.; Bobirică, L.; Râpă, M.; Matei, E.; Predescu, A.M.; Orbeci, C. Photocatalytic Degradation of Ampicillin Using PLA/TiO_2 Hybrid Nanofibers Coated on Different Types of Fiberglass. *Water* **2020**, *12*, 176. [CrossRef]
56. Elsalamony, R.A.; Mahmoud, S.A. Preparation of nanostructured ruthenium doped titania for the photocatalytic degradation of 2-chlorophenol under visible light. *Arab. J. Chem.* **2017**, *10*, 194–205. [CrossRef]
57. Harja, M.; Sescu, A.M.; Favier, L.; Lutic, D.; Ciobanu, G. Photodegradation of rhodamine 6G in presence of Ag/TiO_2 photocatalyst. *Proc. Book Sect. Sustain. Environ. Technol.* **2018**. [CrossRef]
58. Iliev, V.; Tomova, D.; Rakovsky, S. Nanosized N-doped TiO_2 and gold modified semiconductors—Photocatalysts for combined UV-visible light destruction of oxalic acid in aqueous solution. *Desalination* **2010**, *260*, 101–106. [CrossRef]
59. Begum, T.; Gogoi, P.K.; Bora, U. Photocatalytic degradation of crystal violet dye on the surface of Au doped TiO_2 nanoparticle. *Indian J. Chem. Technol.* **2017**, *24*, 97–101.
60. Bai, X.; Lv, L.; Zhang, X.; Hua, Z. Synthesis and photocatalytic properties of palladium-loaded three dimensional flower-like anatase TiO_2 with dominant {0 0 1} facets. *J. Colloid Interface Sci.* **2016**, *467*, 1–9. [CrossRef]
61. Yu, H.; Wang, X.; Sun, H.; Huo, M. Photocatalytic degradation of malathion in aqueous solution using an $Au\text{-}Pd\text{-}TiO_2$ nanotube film. *J. Hazard. Mater.* **2010**, *184*, 753–758. [CrossRef]
62. Loganathan, K.; Bommusamy, P.; Muthaiahpillai, P.; Velayutham, M. The syntheses, characterizations, and photocatalytic activities of silver, platinum, and gold doped TiO_2 nanoparticles. *Environ. Eng. Res.* **2011**, *16*, 81–90. [CrossRef]
63. Mehrjouei, M.; Müller, S.; Möller, D. Catalytic and photocatalytic ozonation of tert-butyl alcohol in water by means of falling film reactor: Kinetic and cost-effectiveness study. *Chem. Eng. J.* **2014**, *248*, 184–190. [CrossRef]
64. Urkude, K.; Thakare, S.R.; Gawande, S. An energy efficient photocatalytic reduction of 4-nitrophenol. *J. Environ. Chem. Eng.* **2014**, *2*, 759–764. [CrossRef]
65. Andronic, L.; Isac, L.; Miralles-Cuevas, S.; Visa, M.; Oller, I.; Duta, A.; Malato, S. Pilot-plant evaluation of TiO_2 and TiO_2-based hybrid photocatalysts for solar treatment of polluted water. *J. Hazard. Mater.* **2016**, *320*, 469–478. [CrossRef] [PubMed]
66. Borges, M.E.; Sierra, M.; Cuevas, E.; García, R.D.; Esparza, P. Photocatalysis with solar energy: Sunlight—Responsive photocatalyst based on TiO_2 loaded on a natural material for wastewater treatment. *Sol. Energy* **2016**, *135*, 527–535. [CrossRef]
67. Sescu, A.M.; Harja, M.; Favier, L.; Berthou, L.O.; de Castro, C.G.; Pui, A.; Lutic, D. Zn/La Mixed Oxides Prepared by Coprecipitation: Synthesis, Characterization and Photocatalytic Studies. *Materials* **2020**, *13*, 4916. [CrossRef]
68. Barzan, M.; Hajiesmaeilbaigi, F. Investigation the concentration effect on the absorption and fluorescence properties of Rhodamine 6G dye. *Optik* **2018**, *159*, 157–161. [CrossRef]